

RESEARCH ARTICLE

Analysis of anti-apoptotic PVT1 oncogene and apoptosis-related proteins (p53, Bcl2, PD-1, and PD-L1) expression in thyroid carcinoma

Afaf T. Ibrahim^{1,2}  | Amin K. Makhdoom³  | Khalid S. Alanazi³  |
Abdulaziz M. Alanazi³  | Abdulaziz M. Mukhle³  | Saad H. Elshafey⁴ |
Eman A. Toraih^{5,6}  | Manal S. Fawzy^{7,8} 

¹Department of Pathology, Faculty of Medicine, Northern Border University, Arar, Saudi Arabia

²Department of Pathology, Faculty of Medicine, Mansoura University, Mansoura, Egypt

³Faculty of Medicine, Northern Border University, Arar, Saudi Arabia

⁴Department of Anatomy, Faculty of Medicine, Northern Border University, Arar, Saudi Arabia

⁵Division of Endocrine and Oncologic Surgery, Department of Surgery, School of Medicine, Tulane University, New Orleans, Louisiana, USA

⁶Genetics Unit, Histology and Cell Biology Department, Faculty of Medicine, Suez Canal University, Ismailia, Egypt

⁷Department of Biochemistry, Faculty of Medicine, Northern Border University, Arar, Saudi Arabia

⁸Department of Medical Biochemistry and Molecular Biology, Faculty of Medicine, Suez Canal University, Ismailia, Egypt

Correspondence

Manal S. Fawzy, Department of Medical Biochemistry, Faculty of Medicine, Northern Border University, Arar, Saudi Arabia.

Email: manal.darwish@nbu.edu.sa

Eman A. Toraih, Division of Endocrine and Oncologic Surgery, Department of Surgery, School of Medicine, Tulane University, New Orleans, Louisiana, USA.

Email: etoraih@tulane.edu

Funding information

Deanship of Scientific Research, Northern Border University, Arar, Saudi Arabia, Grant/Award Number: 7798-MED-2018-3-9-F

Abstract

Background: An aberrant expression of long non-coding RNA PVT1 has been associated with apoptosis in various cancer types. We aimed to explore the PVT1 and four apoptosis-related proteins (p53, Bcl2, and PD-1/PD-L1) signature in thyroid cancer (TC).

Methods: The PVT1 expression level was measured in 64 FFPE TC paired samples by real-time quantitative PCR. Overall and stratified analyses by different clinicopathological features were done. The apoptotic proteins were evaluated by immunohistochemistry staining.

Results: Overall analysis showed significant PVT1 upregulation in TC tissues ($p < 0.001$). Similarly, subgroup analysis by $BRAF^{V600E}$ mutation showed consistent results. Lower expression of p53 was associated with mortality ($p = 0.001$). Bcl2 overexpression was associated with greater tumor size ($p = 0.005$). At the same time, HCV-positive cases were associated with repressed Bcl2 expression levels (54.3% in HCV-negative vs. 6.9% in HCV-positive cases, $p = 0.011$). PD-1 expression was associated with lymph node metastasis ($p = 0.004$). Enhanced PD-L1 expression in the tumor was associated with a higher tumor stage, lymphovascular invasion, and mortality risk. Kaplan–Meier curves for overall survival showed that low p53 and

Clinical trial registration: Not applicable.

This is an open access article under the terms of the [Creative Commons Attribution-NonCommercial](https://creativecommons.org/licenses/by-nc/4.0/) License, which permits use, distribution and reproduction in any medium, provided the original work is properly cited and is not used for commercial purposes.

© 2022 The Authors. *Journal of Clinical Laboratory Analysis* published by Wiley Periodicals LLC.

high PD-L1 expressions were associated with lower survival time. The p53-positive staining is associated with a 90% decreased mortality risk (HR = 0.10, 95%CI = 0.02–0.47, $p = 0.001$), while patients with high PD-L1 were five times more likely to die (HR = 4.74, 95%CI = 1.2–18.7, $p = 0.027$).

Conclusion: Our results confirm the upregulation of PVT1 in TC. The apoptosis-related proteins (p53, Bcl2, and PD-1/PD-L1) showed different prognostic utility in TC patients; in particular, low p53 and high PD-L1 expressions associated with low survival times. Further large-scale and mechanistic studies are warranted.

KEYWORDS

Bcl2, immunohistochemistry, P53, papillary thyroid cancer, PD-1, PD-L1, PVT1, real-time PCR

1 | INTRODUCTION

Thyroid cancer (TC) is the most common endocrine tumor worldwide.¹ Understanding the pathogenesis of TC and finding biomarkers for its early diagnosis and effective treatment are current focal points of research.^{2–4} Accumulating evidence indicates that several protein-coding and non-coding genes play essential roles in TC development and progression.^{2,5–8}

Long non-coding RNAs (lncRNA), a group of endogenous cellular transcripts more than 200 nucleotides in length, have been involved in multiple pathophysiological processes of the human body, especially tumorigenesis and progression of cancers.⁹ The aberrant expression of lncRNA processes crucial functions involved in proliferation, apoptosis, and metastasis through abnormal regulation of gene expression transcriptionally and post-transcriptionally.¹⁰ Given the high tissue specificity, efficiency, and stability, lncRNAs might be used as biomarkers for diagnosis/prognosis or monitoring of human cancers.¹¹

In the last decade, the lncRNA plasmacytoma variant translocation 1 (PVT1) has gained significant attention due to being verified to mediate tumorigenesis in multiple cancers. PVT1 gene, also named as MIR1204HG, MYC Activator, LINC00079, and Onco-lncRNA-100, is located on chromosome 8q24.21, 100 to 500 kb 3-prime of MYC, hosting four microRNAs gene cluster, namely MIR1204, 1205, 1206, 1207, and 1208, and can have 176 splice variant transcripts of varying length (<https://www.ncbi.nlm.nih.gov/gene/5820>). Deregulated expression of PVT1 has been demonstrated to be associated with solid organ^{12–14} and hematological malignancies,¹⁵ and its deregulation could be related to survival and prognosis of cancer patients.^{16–18} Pertinent to clinical practice, PVT1 might act as a prognostic biomarker for tumors and serve as a potential target for therapy.¹⁹

In some tumors, PVT1 was related to apoptosis, as evident in colorectal cancer¹⁶ and malignant pleural mesothelioma.²⁰ Tetracycline-inducible shRNA targeting PVT1 inhibited cell growth and induced apoptosis in bladder cancer cells.²¹ Similarly, PVT1 knockdown affected proliferation and promoted apoptosis of uveal melanoma

cells by inhibiting the "enhancer of zeste homolog 2 (EZH2)" protein.²² In lung squamous cell carcinoma, knockdown of PVT1 inhibited LUSC cell growth.²³ However, the underlying molecular role of PVT1 in thyroid cancer (TC) is still in its infancy.

Previous studies identified the potential mutual relation of PVT1 with some apoptosis-related coding genes expression in cancer tissues, including the p53,^{24,25} Bcl2,²⁶ and PD-1/PD-L1.²⁷ Given that PVT1 represents a promising novel biomarker for various cancer types and has a great potential to be effectively used in clinical practice in the near future, exploring its role in thyroid cancer will add to the knowledge. Here, we aimed to identify the relative expression of PVT1 and four apoptosis-related proteins (p53, Bcl2, PD-1, and PD-L1) expression signature in thyroid cancer compared to paired non-cancer tissues using real-time PCR and immunohistochemistry, respectively. Furthermore, the association of this signature with different clinicopathological parameters of TC patients was investigated.

2 | SUBJECTS AND METHODS

2.1 | Specimen collection

A total of 128 thyroid specimens (64 cancer tissues and their paired non-cancer adjacent tissues) were included in the current analysis. Formalin-fixed paraffin-embedded (FFPE) archival samples were retrieved from Mansoura and Suez Canal University Pathology Labs, Egypt. The "Declaration of Helsinki" guidelines were followed in this work. Ethical approval was provided by the Medical Research Ethics Committee, Faculty of Medicine, Suez Canal University, Egypt. Patient information was collected and managed using anonymous codes. Patients were 18–60 years old and underwent thyroidectomy and/or lobectomy. Patients with the following criteria were excluded: under 18 years old, with non-papillary TC, secondary carcinoma, missing clinical data, loss of follow-up, unmatched cohorts, no available archival paraffin blocks, and/or blocks with insufficient tissue to do complete immunohistochemical staining.

2.2 | Histopathological analysis

A histopathological expert assessed the specimens to confirm the diagnosis and discriminate between cancer and non-cancer regions. FFPE blocks were cut into sections of 4-micron thickness, stained with H&E, examined for tumor diagnosis, and evaluated for other microscopic parameters, such as histological subtype, the staging of cancer, stromal lymphocytes, extra-thyroid extension, lymph node metastasis, lymphovascular and perineural invasion. The TNM (tumor, node, and metastasis) classification of the "American Joint Committee on Cancer (AJCC, 8th edition)" was applied for tumor staging".²⁸

2.3 | Clinical assessment and follow-up

Patient information was obtained from medical records. They included patients' demographic data, primary cancer site, pathology reports, and treatment modalities (surgery, radioactive iodine therapy, and thyroxin intake). Post-thyroidectomy, patients have monitored every six months in which they underwent clinical examination, imaging studies, and serum thyroglobulin level estimation. Relapse, recurrence, and death were reported at follow-up.

2.4 | Gene expression analysis

Qiagen RNeasy FFPE Kit (Cat. #73504, Qiagen, Hilden, Germany) was used to extract total RNA according to the manufacturer's instructions.²⁹ Quantity and purity of extracted RNA were determined using NanoDrop ND-1000 spectrophotometer (NanoDrop Tech., Inc.). As previously described, complementary DNA (cDNA) was prepared using High-capacity RNA-to-cDNA Synthesis Kit (Cat. #4390779).³⁰ Real-time quantitative polymerase chain reaction (PCR) was followed using Universal Master Mix (Cat. #4440042) and TaqMan assay for PVT1 (Assay ID: Hs00413039_m1, Applied Biosystems, Thermo Fisher Scientific Inc.). Reactions were carried out in a T-Professional Basic, Biometra PCR System (Biometra, Goettingen, Germany) for thermocycler and StepOne™ Real-Time PCR System (Applied Biosystems) for real-time PCR following the supplied manufacturer's instructions. The housekeeping gene "glyceraldehyde 3-phosphate dehydrogenase (GAPDH)" was quantified (Assay ID: Hs02786624_g1) in the samples for normalization of the PCR data. Appropriate negative controls were included in each run (no template and no enzyme samples), and duplicate PCR runs were performed. The "Minimum Information for Publication of Quantitative Real-Time PCR Experiments (MIQE)" guidelines were followed during the experiments.³¹ Fold changes of PVT1 gene expression in each patient's cancer tissue relative to the corresponding non-cancer adjacent tissues (NAT) were estimated via the "Livak method" based on the quantification (threshold) cycle ($C_{q\text{ or }C_T}$) value: relative gene expression = $2^{-\Delta\Delta Cq}$.³²

2.5 | Immunohistochemistry analysis

For *BRAF*^{V600E} mutation analysis, 5 μm thick sections of FFPE tissues were prepared. VE1 IHC method was applied as detailed previously.³³ Normal thyroid tissues were run as a negative control. For apoptosis-related protein expression analysis, the deparaffinized tissue sections were pretreated with hydrogen peroxide (3%) solution and incubated at room temperature for 15 min to remove endogenous peroxidase. Antigen retrieval was performed in sodium citrate buffer solution for 5 min using a microwave oven, followed by automatic cooling at room temperature. Then tissues were incubated with primary antibodies as follows: Anti-p53 antibodies (a rabbit polyclonal antibody IgG (clone YPA2006; Chongqing Biopsies CO., Ltd.) with dilution 1:200 and pH 7.4, Anti-Bcl2 antibodies (Mouse monoclonal anti-Bcl2. CELL MARQUE, code No 226 M-98, 7 ml prediluted, anti-PD-L1 (Clone, YPA1638, Biospes, Chongqing Biospes Co., Ltd.), and anti-PD-1 (Clone, YPA1637, Biospes, Chongqing Biospes Co., Ltd.). The whole tissue was covered with antibodies and incubated 8 h in a refrigerator at 4°C. For secondary antibody incubation, tissue samples were incubated with the streptavidin-biotin complex method using a SAB-PO kit (Nichirei, Tokyo, Japan) at room temperature for one hour. Antigen detection was carried out by placing diaminobenzidine on each section. The slides were counterstained with hematoxylin and dehydrated in alcohol and xylene before mounting slides. For negative controls, sections were treated the same way, but they were incubated with antibody diluent instead of the primary antibody. Positive controls were used parallel (colon cancer for p53; Tonsil tissue for PD-1 and PD-L1). The photos were obtained using a Nikon magnifying lens prepared with a 5-megapixel cooled CCD camera joined with the Picture Pro Plus AMS7 computer program.

2.6 | Interpretation of immunohistochemical results

An expert pathologist has assessed the immunostained slides blindly to the clinicopathological features. For p53, if more than 25% of tissue were stained, it was considered a p53 positive sample. For Bcl2, it scored negative if $\leq 5\%$ of neoplastic cells were stained and considered positive if scored from 6% to 100%. The value of Bcl2 was considered low expression if 6 to less than 50% were brown stained and high expression if $\geq 50\%$ of tumor cells were brown stained.³⁴

Regarding the positive immunostaining of PD-1 and PD-L1 in the tumor cells and immune cells, the intensity of the stain was scored as 0 (no staining), 1 (light yellow), 2 (brown), and 3 (deep brown). The number of stained cells per 100 was scored as 1 ($\leq 10\%$), 2 (10% ~ 50%), and 3 ($\geq 50\%$). High PD-L1 expression was detected when the staining strength score was multiplied, and the number of stained cells per 100 cells was no less than three. Regarding immune cell-specific PD-L1 and PD-1 expression, the percentage of stained cells per 100 cells was detected and categorized as 0%–9%,

10%–49%, and 50–100% stained immune cells. Therefore, >50% was used as a cutoff for high expression for PD-1 and PD-L1.^{35,36}

2.7 | Statistical analysis

Data were managed using the "Statistical Package for the Social Sciences (SPSS) for Windows" software (version 22.0), BioVinci (version 1.1.3), R version 3.5.3, and R studio version 1.1.383. Categorical variables were compared using the chi-square (χ^2) or Fisher's exact tests where appropriate, while the student's *t*-test or Mann-Whitney *U* tests were used to compare continuous variables. Log Rank (Mantel-Cox) test was used to estimate the overall survival (OS) time defined as "the interval between the time of surgery to death or the last follow-up," and the disease-free survival (DFS) time defined as "the time length that the patient survives after primary cancer treatment ends without any signs/symptoms of that cancer" of TC patients. Meanwhile, Kaplan–Meier survival curves were generated for the OS and DFS. Multivariate Cox regression analysis was applied to identify predictors for mortality. A two-tailed *p*-value of <0.05 was considered significant.

3 | RESULTS

3.1 | Characteristics of the study population

A total of 64 patients with up to a 7-years follow-up period were included in the current study. Of these, 70.3% were younger than 55 years old, 78.1% were females, and 43.7% were *BRAF* mutant. There were no significant clinical or pathological differences between patients with *BRAF* mutant and *BRAF* wild types (Table 1).

3.2 | PVT1 gene expression level

The overall analysis of 64 paired tissues showed upregulation of the PVT1 gene in cancer tissues compared to paired adjacent non-cancer tissues ($p < 0.001$). Similarly, subgroup analysis by *BRAF* mutation showed consistent results (Figure 1). PVT1 upregulation was observed in 73.8% ($N = 48$) of cases. Otherwise, PVT1 expression was not associated with clinical or pathological features (Table 2).

3.3 | Apoptosis-related protein expression

Immunohistochemistry reactivity is shown in Figures 2 and 3. Positive staining of p53 was observed in 51 cases (79.6%). Bcl2 protein expression was found in 35 samples (54.6%). At the same time, PD-1 and PD-L1 were positively stained in 52 (81.3%) and 18 (28.1%) patients, respectively (Figure S1). As depicted in Table 3, females were more likely to have higher p53 protein staining than males (84.3% vs. 15.7%, $p = 0.030$). Lower expression of p53 was associated with

mortality (53.8% vs. 7.8% in high expressors, $p = 0.001$). Protein expression of the anti-apoptotic Bcl2 varied across histopathological variants ($p = 0.012$). Overexpression was associated with greater tumor size (58.6% vs. 22.9%, $p = 0.005$), while HCV-positive cases were associated with repressed expression levels (54.3% in HCV negative vs. 6.9% in HCV positive, $p = 0.011$). PD-1 protein was associated with lymph node metastasis (63.5% vs. 16.7%, $p = 0.004$). For its ligand, PD-L1 protein, elders (55.6% vs. 19.6%, $p = 0.007$) and males (44.4% vs. 13.0%, $p = 0.015$) were more likely to exhibit higher protein staining. Enhanced PD-L1 expression in tumor was associated with higher tumor stage (72.2% vs. 26.1%, $p = 0.001$), lymphovascular invasion (44.4% vs. 2.2%, $p < 0.001$), and risk of mortality (38.9% vs. 8.7%, $p = 0.008$).

3.4 | Survival analysis

As depicted in Figure 4, none of the gene or protein markers were associated with disease-free survival. However, Kaplan–Meier curves for overall survival showed that low p53 ($p < 0.001$) and high PD-L1 ($p = 0.018$) protein expression were associated with lower survival times. Mean survival times for each group are demonstrated in Table 4. p53 protein-positive staining is associated with a 90% decreased risk of mortality (HR = 0.10, 95%CI = 0.02–0.47, $p = 0.001$), while patients with high PD-L1 were five times more likely to die (HR = 4.74, 95%CI = 1.2–18.7, $p = 0.027$) (Figure 5).

4 | DISCUSSION

Accumulating evidence has confirmed the close relation of deregulated lncRNAs expression signature with the biological behavior of TC.³⁷ In this study, we selected the lncRNA PVT1 and four anti-apoptotic proteins to determine their expression signature in TC tissues to improve our understanding of their roles in TC and their potential diagnostic and/or prognostic utility in this type of cancer. We found that PVT1 was upregulated in TC samples compared to non-cancer tissues by overall analysis and stratified analysis by the presence of *BRAF*^{V600E} mutation. This finding is congruent with the oncogenic role that PVT1 plays in several cancers, including TC.^{37,38}

The gene of PVT1 resides in a well-known cancer risk-related locus on "chromosome 8q24," which could partly explain the high potential of dysregulated gene expression to be associated with the development and progression of multiple cancers.³⁹ The oncogenic role of PVT1 has been reported in several tumors, such as lung,⁴⁰ gallbladder,⁴¹ colon,^{42,43} hepatocellular,^{44,45} breast,⁴⁶ and ovarian⁴⁷ cancers.

The impact of PVT1 on cancer cell behaviors appears to be mediated via an interlinked network of other non-coding RNAs, molecular mediators, and regulatory proteins.^{48,49} For example, PVT1 was reported to increase Mcl-1 (an apoptosis regulator and anti-apoptotic factor) transcript levels by promoting its stability in renal cell carcinoma.⁵⁰ It could promote proliferation and tumorigenesis

TABLE 1 Characteristics of study population according to *BRAF*^{V600E} mutation

Patient Characteristics	Levels	Total (N = 64)	<i>BRAF</i> wild type (N = 36)	<i>BRAF</i> mutant (N = 28)	p-value
Demographic data					
Age, years	<55 y	45 (70.3)	25 (69.4)	20 (71.4)	0.86
	≥55 y	19 (29.7)	11 (30.6)	8 (28.6)	
Sex	Male	14 (21.9)	7 (19.4)	7 (25)	0.76
	Female	50 (78.1)	29 (80.6)	21 (75)	
Pathological assessment					
Laterality	Unilateral	47 (73.4)	26 (72.2)	21 (75)	0.80
	Bilateral	17 (26.6)	10 (27.8)	7 (25)	
Histological variant	Classical	32 (50)	21 (58.3)	11 (39.3)	0.16
	Follicular	24 (37.5)	13 (36.1)	11 (39.3)	
	Oncocytic	2 (3.1)	0 (0)	2 (7.1)	
	Tall cell	6 (9.4)	2 (5.6)	4 (14.3)	
Pathology Stage	Stage I	48 (75)	28 (77.8)	20 (71.4)	0.72
	Stage II	5 (7.8)	3 (8.3)	2 (7.1)	
	Stage IVB	11 (17.2)	5 (13.9)	6 (21.4)	
T stage	T1	15 (23.4)	7 (19.4)	8 (28.6)	0.41
	T2	24 (37.5)	16 (44.4)	8 (28.6)	
	T3	25 (39.1)	13 (36.1)	12 (42.9)	
N stage	N0	29 (45.3)	17 (47.2)	12 (42.9)	0.92
	N1a	16 (25)	9 (25)	7 (25)	
	N1b	19 (29.7)	10 (27.8)	9 (32.1)	
M stage	M0	53 (82.8)	31 (86.1)	22 (78.6)	0.51
	M1	11 (17.2)	5 (13.9)	6 (21.4)	
Focality	Unifocal	40 (62.5)	20 (55.6)	20 (71.4)	0.29
	Multifocal	24 (37.5)	16 (44.4)	8 (28.6)	
Extrathyroidal extension	Negative	53 (82.8)	31 (86.1)	22 (78.6)	0.51
	Positive	11 (17.2)	5 (13.9)	6 (21.4)	
Lymphovascular invasion	Negative	55 (85.9)	32 (88.9)	23 (82.1)	0.48
	Positive	9 (14.1)	4 (11.1)	5 (17.9)	
Perineural invasion	Negative	62 (96.9)	35 (97.2)	27 (96.4)	0.85
	Positive	2 (3.1)	1 (2.8)	1 (3.6)	
Lymphocyte enrichment	Negative	33 (51.6)	16 (44.4)	17 (60.7)	0.21
	Positive	31 (48.4)	20 (55.6)	11 (39.3)	
HCV antibody	Negative	43 (67.2)	27 (75)	16 (57.1)	0.18
	Positive	21 (32.8)	9 (25)	12 (42.9)	
Intervention					
Thyroidectomy	Unilateral	9 (14.1)	4 (11.1)	5 (17.9)	0.48
	Total/subtotal	55 (85.9)	32 (88.9)	23 (82.1)	
Neck dissection	Negative	18 (28.1)	10 (27.8)	8 (28.6)	0.94
	Positive	46 (71.9)	26 (72.2)	20 (71.4)	
Residual after resection	Negative	37 (57.8)	19 (52.8)	18 (64.3)	0.44
	Positive	27 (42.2)	17 (47.2)	10 (35.7)	
Received Eltroxin	Negative	30 (46.9)	15 (41.7)	15 (53.6)	0.45
	Positive	34 (53.1)	21 (58.3)	13 (46.4)	

(Continues)

TABLE 1 (Continued)

Patient Characteristics	Levels	Total (N = 64)	BRAF wild type (N = 36)	BRAF mutant (N = 28)	p-value
RAI	Negative	36 (56.3)	17 (47.2)	19 (67.9)	0.13
	Positive	28 (43.8)	19 (52.8)	9 (32.1)	
EBRT	Negative	59 (92.2)	35 (97.2)	24 (85.7)	0.15
	Positive	5 (7.8)	1 (2.8)	4 (14.3)	
Follow-up					
Progression	Negative	35 (54.7)	18 (50)	17 (60.7)	0.45
	Positive	29 (45.3)	18 (50)	11 (39.3)	
Mortality	Survived	53 (82.8)	29 (80.6)	24 (85.7)	0.74
	Died	11 (17.2)	7 (19.4)	4 (14.3)	

Note: Data are represented as frequency (percentage).

Abbreviations: RAI: Radioactive iodine, EBRT: External beam radiotherapy, Progression: included recurrence, relapse, and distant metastasis. A two-sided Chi-square test was applied. Statistical significance was set at p -value <0.05 .

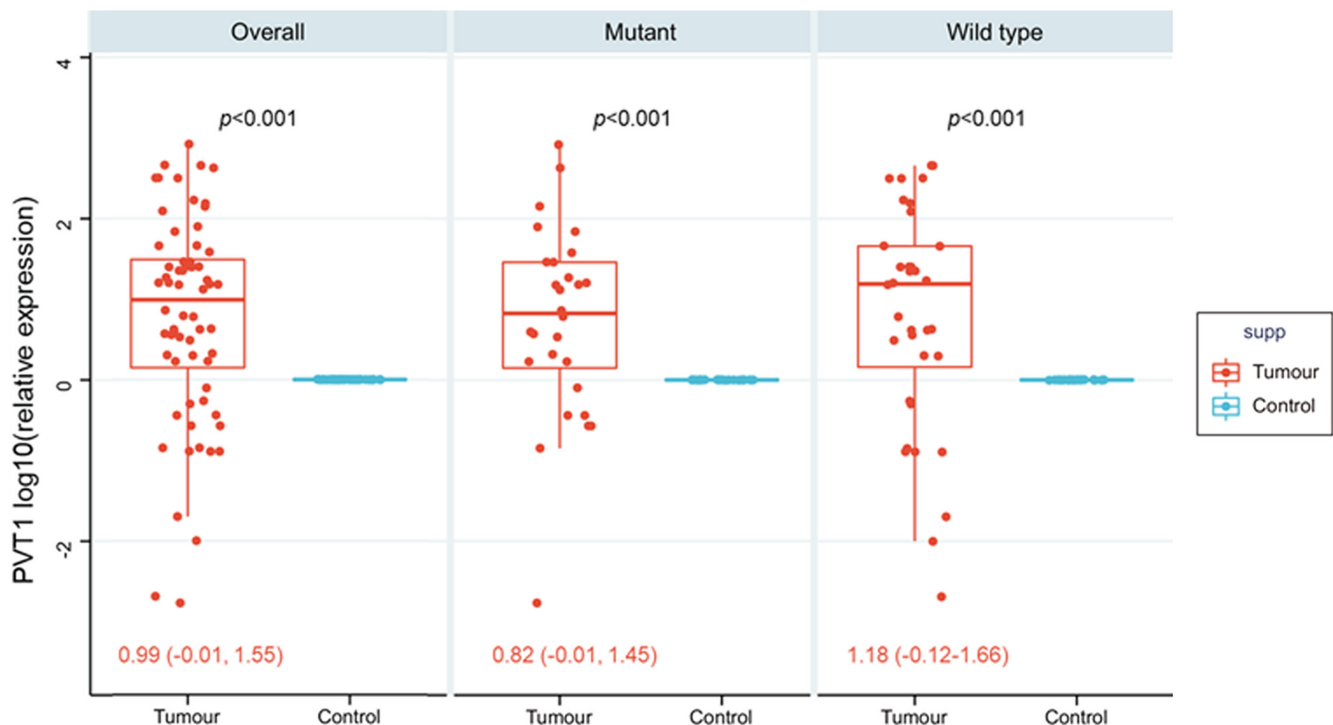


FIGURE 1 PVT1 gene expression profile in thyroid cancer tissues compared to normal counterparts. Paired t-test was used to compare cancer and non-cancer tissues. Overall analysis and stratification by $BRAF^{V600E}$ mutation are shown. All p -values were <0.001 . Fold change was normalized by the $GAPDH$ housekeeping gene. The median and interquartile fold change range of tumor specimens relative to non-cancer paired tissues are shown

in triple-negative breast cancer through the $KLF5/\beta$ -catenin signaling pathway.⁵¹ PVT1 knockdown has been reported to promote apoptosis via transforming growth factor- β signaling activation in the colorectal cancer cell.¹⁶ In TC, PVT1 was found to modulate the proliferation of cancer cells by recruiting the "polycomb enhancer of zeste homolog 2; EZH2" and regulating the "thyroid-stimulating hormone receptor" expression.³⁸ Feng et al. reported that PVT1 could act as a competing endogenous RNA (ceRNA) in papillary TC sponging the microRNA-30a with subsequent upregulation of its target

gene "insulin-like growth factor-1 receptor." In response to PVT1 downregulation, the later researchers found that TC cells apoptosis was promoted with inhibition of cell cycle progression, proliferation, and invasion/migration.⁵²

$BRAF^{V600E}$, a TC-specific gene, is one of the most common mutations that has been linked to papillary TC.⁵³ Although several studies have shown a subtype-specific expression of some lncRNAs in papillary TC stratified by this mutation, such as correlation with NAMA downregulation,⁵⁴ CCND1, PERP, CDKN1A,

TABLE 2 Association of *PVT1* gene expression and clinicopathological characteristics

Characteristics	Levels	Low expression	High expression	p-value
Demographic data				
Age, years	<55 year	13 (81.3)	32 (66.7)	0.35
	≥55 year	3 (18.8)	16 (33.3)	
Sex	Male	2 (12.5)	12 (25)	0.48
	Female	14 (87.5)	36 (75)	
Pathological assessment				
Laterality	Unilateral	12 (75)	35 (72.9)	0.87
	Bilateral	4 (25)	13 (27.1)	
Histological variant	Classical	8 (50)	24 (50)	0.77
	Follicular	7 (43.8)	17 (35.4)	
	Oncocytic	0 (0)	2 (4.2)	
	Tall cell	1 (6.3)	5 (10.4)	
Pathology Stage	Stage I/II	15 (93.8)	38 (79.2)	0.83
	Stage IVB	1 (6.3)	10 (20.8)	
Tumor size	T1/2	9 (56.3)	30 (62.5)	0.48
	T3	7 (43.8)	18 (37.5)	
LN metastasis	Positive	8 (50)	27 (56.3)	0.79
Distant metastasis	Positive	1 (6.3)	10 (20.8)	0.26
Focality	Multifocal	4 (25)	20 (41.7)	0.37
ETE	Positive	2 (12.5)	9 (18.8)	0.71
LVI	Positive	4 (25)	5 (10.4)	0.21
Lymphocyte enrichment	Positive	8 (50)	23 (47.9)	0.88
<i>BRAF</i> ^{V600E}	Mutant	7 (43.8)	21 (43.8)	0.99
HCV antibody	Positive	2 (12.5)	19 (39.6)	0.06
Follow-up				
Progression	Positive	6 (37.5)	23 (47.9)	0.56
Mortality	Died	2 (12.5)	9 (18.8)	0.71

Note: Data are represented as frequency (percentage).

Abbreviations: ETE: Extrathyroidal extension; LN: lymph node; LVI: Lymphovascular invasion.

Progression: included recurrence, relapse, and distant metastasis. A two-sided Chi-square test was used. Statistical significance was set at p-value <0.05.

ZMAT3, and THBS1 upregulation,⁵⁵ ENS-653 overexpression,⁵⁶ the antisense lncRNA COMET expression,⁵⁷ and the lncRNAs AACS, *ALDH3B1*, *ITPR3*, *LAD1*, *MMD*, *RASA1* and *PVRL3* gene induction,⁵⁸ we did not explore a significant difference of the *PVT1* expression levels between patients with TC stratified according to this type of mutation. This finding will require further confirmation by replication studies, including a larger sample size with variable TC histopathological subtypes.

On exploring the prognostic utility of the selected apoptosis-related protein expression signatures in TC, the authors found that p53-positive staining was associated with a 90% decreased risk of mortality. This finding aligns with the tumor suppressor functions of p53 that have long been recognized.⁵⁹ Moreover, it has been found that high expression of *PVT1* in cancer cells is associated with *EZH2* and *MDM2* overexpression that downregulates p53 protein expression, contributing to tumorigenesis.⁶⁰ Otherwise, DNA damage and

oncogenic stress could activate p53 to bind specific DNA response elements of the target genes. In TC, the tumor suppressor activity of p53 could be inhibited at the transcriptional, post-translational protein stability, and/or downstream-signaling level.⁶¹ For example, downregulation of the "AT-hook containing zinc finger protein 1 (PATZ1)" in TC can impact p53 binding to its responsive elements, favoring cell migration and epithelial-to-mesenchymal transition (EMT) as proposed by Chiappetta et al..⁶² Other reported molecular mechanisms as the downregulation of "Abraxas brother 1 (ABRO-1)" that cleaves "Lys-63-linked ubiquitin" and upregulation of the proto-oncogene "PTTG1-Binding Factor (PBF)" in TC enhance p53 polyubiquitination and decrease its stability.^{63,64} Also, some "Murine double minute (MDM-S and MDM4-211)," truncated MDM4 spliced variants expressed in TC, were reported to be potent negative regulators to p53 in vitro.⁶⁵ All the previous reports confirm the essential role that p53 could play in the early stages of thyroid tumorigenesis

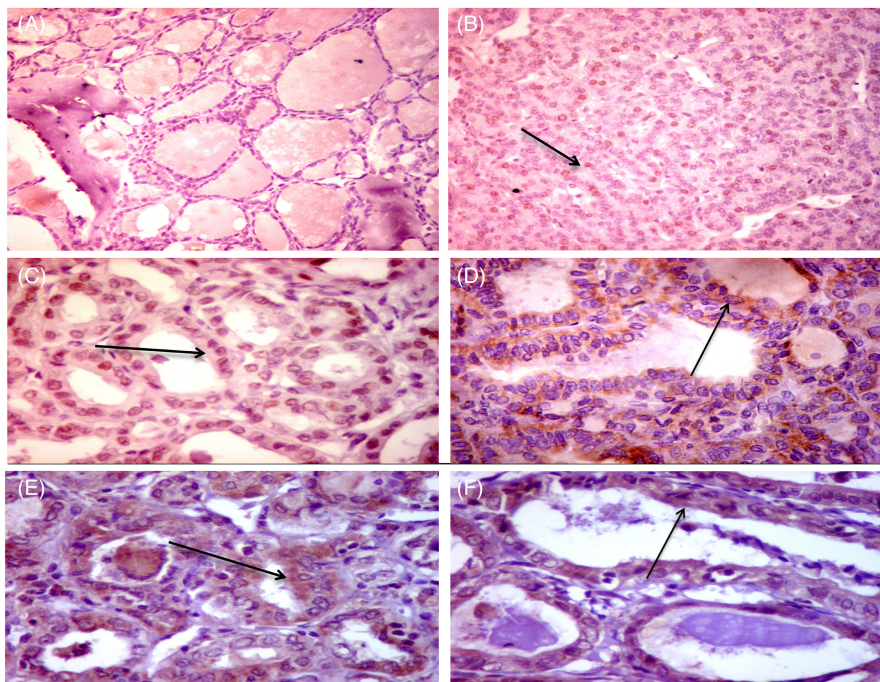


FIGURE 2 Immunohistochemical (IHC) staining for p53 and BCL2 proteins in papillary thyroid carcinoma (PTC). IHC staining for p53 protein showed negative staining in non-cancerous thyroid tissue (AX200) and scattered nuclear staining for p53 in PTC (Black arrow) (BX200). Diffuse nuclear staining for p53 in follicular variant of PTC (black arrow) (CX400). Staining for BCL2 protein showed focal mild cytoplasmic staining for BCL2 in hyperplastic nodule (DX 400), diffuse strong cytoplasmic staining for BCL2 in follicular variant of PTC (black arrow) (EX400), and moderate cytoplasmic staining in PTC (FX400)

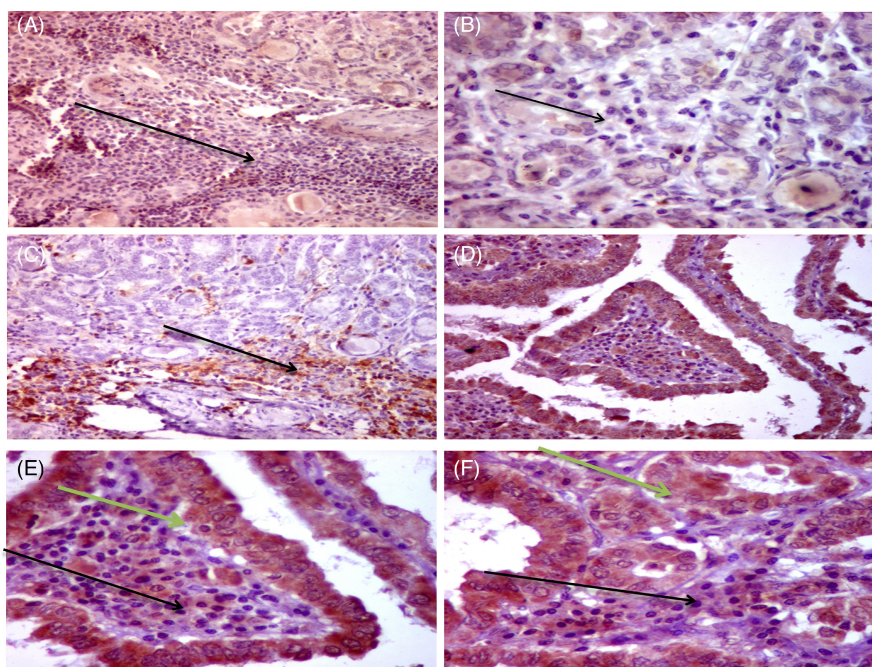


FIGURE 3 Immunohistochemical (IHC) staining for PD-1 and PD-L1 in papillary thyroid carcinoma (PTC). Thyroid papillary carcinoma follicular variant with dense intra-tumoral immune cells (yellow arrow) showed negative staining of PD-1 protein in intracutaneous immune cells (ICCs) of PTC (AX100). Higher power of the same case showed negative staining for PD-1 in ICCs (black arrow) (BX200). Positive staining of PD-1 protein in ICCs in follicular variant of PTC (Black arrow) (CX100). Diffuse positive staining for PD-L1 protein in both tumor cells and intra-tumoral immune cells in PTC (classic variant) (DX200). Higher power of the same case (D) showed diffuse strong cytoplasmic staining of all tumor cells (green arrows) and most of the ICCs for PD-L1 (black arrows) (EX400). A follicular variant of PTC showed diffuse positive staining for PD-L1 in tumor (green arrow) and immune cells (black arrow) (FX400)

and support its significant association with better survival in the current TC cases.

Our findings also indicate that overexpression of the anti-apoptotic Bcl2 was associated with greater tumor size, and its

repressed expression levels were evident in HCV-positive cases. Bcl2 protein family has been reported to play a crucial role in the pathophysiology of TC derived from follicular epithelium by disturbing the proapoptotic/anti-apoptotic events equilibrium.⁶⁶ Its

TABLE 3 Association of protein expression levels and clinicopathological features

Characteristics	Levels	p53		bcl2		PD-1		PD-L1 (Tumor)		PD-L1 (lymphocyte)	
		Low expression	High expression	Low expression	High expression						
Demographic data											
Age, years	<55 y	7 (53.8)	38 (74.5)	27 (77.1)	18 (62.1)	10 (83.3)	35 (67.3)	37 (80.4)	8 (44.4)**	23 (69.7)	22 (71)
	≥55 y	6 (46.2)	13 (25.5)	8 (22.9)	11 (37.9)	2 (16.7)	17 (32.7)	9 (19.6)	10 (55.6)	10 (30.3)	9 (29)
Sex	Male	6 (46.2)	8 (15.7)*	7 (20)	7 (24.1)	1 (8.3)	13 (25)	6 (13)	8 (44.4)*	8 (24.2)	6 (19.4)
	Female	7 (53.8)	43 (84.3)	28 (80)	22 (75.9)	11 (91.7)	39 (75)	40 (87)	10 (55.6)	25 (75.8)	25 (80.6)
Pathological assessment											
Laterality	Unilateral	7 (53.8)	40 (78.4)	25 (71.4)	22 (75.9)	9 (75)	38 (73.1)	33 (71.7)	14 (77.8)	24 (72.7)	23 (74.2)
	Bilateral	6 (46.2)	11 (21.6)	10 (28.6)	7 (24.1)	3 (25)	14 (26.9)	13 (28.3)	4 (22.2)	9 (27.3)	8 (25.8)
Histological variant	Classical	8 (61.5)	24 (47.1)	22 (62.9)	10 (34.5)*	3 (25)	29 (55.8)	24 (52.2)	8 (44.4)	15 (45.5)	17 (54.8)
	Follicular	3 (23.1)	21 (41.2)	7 (20)	17 (58.6)	6 (50)	18 (34.6)	15 (32.6)	9 (50)	15 (45.5)	9 (29)
Pathology Stage	Oncocytic	0 (0)	2 (3.9)	1 (2.9)	1 (3.4)	1 (8.3)	1 (1.9)	2 (4.3)	0 (0)	1 (3)	1 (3.2)
	Tall cell	2 (15.4)	4 (7.8)	5 (14.3)	1 (3.4)	2 (16.7)	4 (7.7)	5 (10.9)	1 (5.6)	2 (6.1)	4 (12.9)
Tumor size	Stage I/II	9 (69.2)	44 (86.3)	31 (88.6)	22 (75.9)	12 (100)	41 (78.8)	41 (89.1)	12 (66.7)	24 (72.7)	29 (93.5)
	Stage IVB	4 (30.8)	7 (13.7)	4 (11.4)	7 (24.1)	0 (0)	11 (21.2)	5 (10.9)	6 (33.3)	9 (27.3)	2 (6.5)
LN metastasis	T1/2	9 (69.2)	30 (58.8)	27 (77.1)	12 (41.4)**	9 (75)	30 (57.7)	34 (73.9)	5 (27.8)**	24 (72.7)	29 (93.5)
	T3	4 (30.8)	21 (41.2)	8 (22.9)	17 (58.6)	3 (25)	22 (42.3)	12 (26.1)	13 (72.2)	9 (27.3)	2 (6.5)
Distant metastasis	Positive	7 (53.8)	28 (54.9)	16 (45.7)	19 (65.5)	2 (16.7)	33 (63.5)**	26 (56.5)	9 (50)	17 (51.5)	18 (58.1)
	Negative	4 (30.8)	7 (13.7)	4 (11.4)	7 (24.1)	0 (0)	11 (21.2)	5 (10.9)	6 (33.3)	9 (27.3)	2 (6.5)
Focality	Multifocal	8 (61.5)	16 (31.4)	14 (40)	10 (34.5)	6 (50)	18 (34.6)	20 (43.5)	4 (22.2)	9 (27.3)	15 (48.4)
	Focal	3 (23.1)	8 (15.7)	6 (17.1)	5 (17.2)	0 (0)	11 (21.2)	9 (19.6)	2 (11.1)	3 (9.1)	8 (25.8)
BRAF ^{V600E}	Positive	3 (23.1)	6 (11.8)	2 (5.7)	7 (24.1)	0 (0)	9 (17.3)	1 (2.2)	8 (44.4)**	6 (18.2)	3 (9.7)
	Negative	6 (46.2)	22 (43.1)	18 (51.4)	10 (34.5)	3 (25)	25 (48.1)	20 (43.5)	8 (44.4)	17 (51.5)	11 (35.5)
HCV Ab	Positive	4 (30.8)	17 (33.3)	19 (54.3)	2 (6.9)*	5 (41.7)	16 (30.8)	18 (39.1)	3 (16.7)	10 (30.3)	11 (35.5)
	Negative	7 (53.8)	22 (43.1)	17 (48.6)	12 (41.4)	6 (50)	23 (44.2)	21 (45.7)	8 (44.4)	12 (36.4)	17 (54.8)
Mortality	Progression	7 (53.8)	4 (7.8)**	7 (20)	4 (13.8)	3 (25)	8 (15.4)	4 (8.7)	7 (38.9)**	7 (21.2)	4 (12.9)
	Died	7 (53.8)	4 (7.8)**	7 (20)	4 (13.8)	3 (25)	8 (15.4)	4 (8.7)	7 (38.9)**	7 (21.2)	4 (12.9)

Note: Data are represented as frequency (percentage).

Abbreviations: LN, lymph node; ETE, Extrathyroidal extension; LVI, Lymphovascular invasion; HCV Ab, hepatitis C virus antibody.

Progression: included recurrence, relapse, and distant metastasis. A two-sided Chi-square test was used. Statistical significance of bold values was set at p -value < 0.05, * p < 0.05, ** p < 0.01, *** p < 0.001.

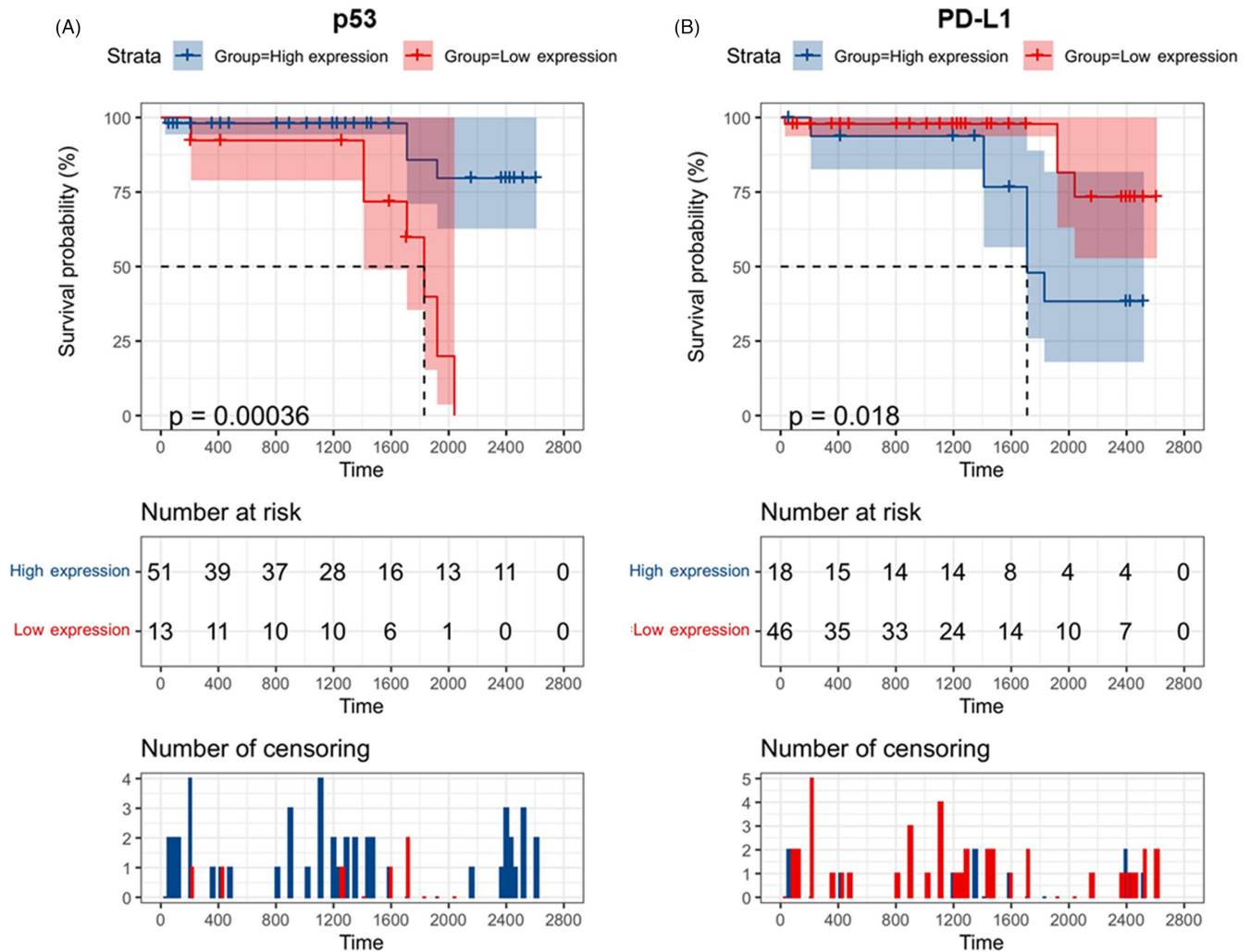


FIGURE 4 Kaplan-Meier curves for overall survival. (A) p53 protein. (B) PD-L1 protein. Log Rank (Mantel-Cox) test was used. Data are presented as mean survival estimates in days

protein expression has been identified in well-differentiated TC subtypes compared to poorly differentiated/undifferentiated ones.⁶⁷ Using mouse models, Du et al. have explored that PVT1-related anti-apoptotic effect and 5-Fu resistance in gastric cancer cases can be mediated through Bcl2 activation, confirming the potential interplay between the two studied biomolecules.²⁶ The observed downregulation of Bcl2 protein expression in our HCV-positive TC cases compared to negative ones was in line with a previous study done by Visco et al. on another type of cancer.⁷⁴ The researchers compared 44 HCV-positive cases of diffuse large B-cell lymphoma with 132 HCV-negative counterparts. They found that Bcl2 protein was significantly less expressed in the former cohort than the latter, suggesting that modulation of the apoptotic response via Bcl2 interacting domain degradation might be one strategy used by HCV to escape immune surveillance and ensure chronic infectivity.⁶⁸ Meanwhile, HCV nonstructural protein-5A has been found to act as a Bcl2 homolog, interacting with Bax to protect HCC cells against apoptosis.⁶⁹

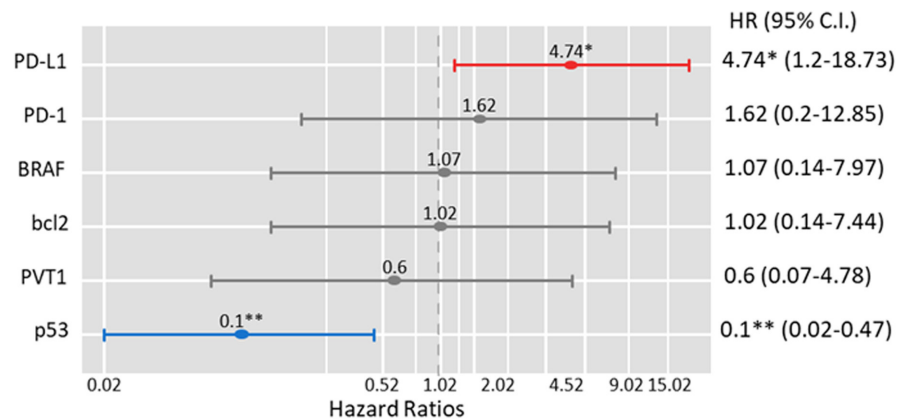
On exploring the involvement of the main "immune-checkpoint" PD-1/PD-L1 in the current TC cases, we found PD-1 protein was associated with lymph node metastasis. Furthermore, enhanced PD-L1 expression in the tumor was associated with poor prognostic indices in terms of higher tumor stage, lymphovascular invasion, and mortality risk, as patients with high PD-L1 protein expression were nearly five times more likely to die. Of clinical relevance, the identified predicting utility of PD-1/PD-L1 to worse prognosis in patients with TC, representing real hope for early implementation of anti-PD-1/PD-L1 immunotherapies, contributing to "thyroid precision oncology".⁷⁰ Consistent with our findings, previous studies also reported the clinical utility of the PD-1/PD-L1 pathway in TC cases with/without autoimmune origin and with variable histopathological types.⁷¹⁻⁸¹ Given the role of PD-L1 in tumor immune escape, its expression (either at the protein or mRNA level) was associated with decreased progression-free survival in patients with papillary TC.^{71,73,81} Using "immunocompromised nude mice," PD-L1 upregulation has been reported to confer a metastatic potential in

TABLE 4 Overall and disease-free survival times of thyroid cancer patients

Biomarker	Expression	Disease-free survival (months)	p-value	Overall survival (months)	p-value
PVT1 gene	Low	48.8 (29.5–68.2)	0.96	69.6 (57.1–82.3)	0.91
	High	49.6 (38.0–61.2)		73.8 (66.9–80.7)	
p53 protein	Low	39.1 (24.6–53.6)	0.71	55.5 (45.8–65.2)	<0.001
	High	51.7 (6.06–39.8)		80.2 (74.2–86.3)	
bcl2 protein	Low	51.7 (38.4–64.9)	0.49	73.5 (65.2–81.7)	0.95
	High	45.4 (30.9–59.9)		71.1 (60.8–81.3)	
PD-1 protein	Low	55.5 (39.1–71.9)	0.58	77.7 (71.7–83.6)	0.28
	High	49.3 (37.1–61.5)		71.5 (62.9–80.1)	
PD-L1 tumor	Low	50.9 (38.8–63.0)	0.73	79.8(73.6–86.1)	0.018
	High	48.5 (30.1–66.8)		62.9 (51.7–74.1)	
PD-L1 lymphocyte	Low	59.7 (45.6–73.7)	0.08	71.9 (62.9–80.9)	0.63
	High	39.6 (26.6–52.5)		71.9 (64.6–79.1)	
BRAF mutation	Negative	41.9 (28.7–55.1)	0.11	72.2 (65.2–79.3)	0.92
	Positive	57.9 (42.4–73.3)		73.1 (61.4–84.7)	

Note: Log Rank (Mantel-Cox) test was used. Data are presented as mean survival estimates in months and 95% confidence interval. Bold values indicate significance at p-value <0.05.

FIGURE 5 Multivariate Cox regression analysis for overall survival. Data are presented as hazard ratio (HR) and 95% confidence interval (C.I.). * $p = 0.027$, ** $p = 0.001$



well-differentiated TC and its silencing delayed follicular TC growth and metastasis.⁸² Interestingly, PD-L1 was also reported to play a role in glycolysis, stemness, cell death resistance, and EMT as a major metastasis pre-requisite.⁸³

5 | CONCLUSION

Collectively, this study confirmed the oncogenic role of the lncRNA PVT1 in TC patients identified by overall and BRAF^{V600E}-stratified analyses. Furthermore, studied apoptosis-related proteins (p53, Bcl2, and PD-1/PD-L1) showed associations with several poor prognostic indices in TC patients; in particular, low p53 and high PD-L1 expressions showed significant association with low overall survival. These findings could support the prognostic utility of the studied apoptosis-related proteins in TC and pave the road toward future personalized therapy. Multicenter studies including a larger sample size of clinical cases, particularly indeterminate lesions, are warranted to validate the findings in other histopathological TC subtypes.

ACKNOWLEDGMENT

The authors would like to acknowledge the approval and the support of this research study by grant No. (MED-2018-3-9-F-798) from the Deanship of Scientific Research, Northern Border University, Arar, Saudi Arabia.

CONFLICT OF INTEREST

The authors report no conflicts of interest.

AUTHOR CONTRIBUTIONS

"All authors contributed to data analysis, drafting, or revising the article, have agreed on the journal to which the article has been submitted, gave final approval of the version to be published, and agree to be accountable for all aspects of the work."

ETHICAL APPROVAL

"Declaration of Helsinki" guidelines were followed in this work. Ethical approval was provided by the Medical Research Ethics Committee, Faculty of Medicine, Suez Canal University, Egypt.

PATIENT CONSENT STATEMENT

Not applicable.

PERMISSION TO REPRODUCE MATERIAL FROM OTHER SOURCES

Not applicable.

DATA AVAILABILITY STATEMENT

"All data generated or analyzed during this study are included in this submitted article and supplementary materials."

ORCID

Afaf T. Ibrahim  <https://orcid.org/0000-0002-8636-0220>

Amin K. Makhdoom  <https://orcid.org/0000-0001-5434-6988>

Khalid S. Alanazi  <https://orcid.org/0000-0002-5169-2524>

Abdulaziz M. Alanazi  <https://orcid.org/0000-0002-0255-5945>

Abdulaziz M. Mukhlef  <https://orcid.org/0000-0001-6409-7153>

Eman A. Toraih  <https://orcid.org/0000-0001-9267-3787>

Manal S. Fawzy  <https://orcid.org/0000-0003-1252-8403>

REFERENCES

- Rossi ED, Pantanowitz L, Hornick JL. A worldwide journey of thyroid cancer incidence centred on tumour histology. *Lancet Diabetes Endocrinol.* 2021;9(4):193-194.
- Yang L, Tan Z, Li Y, et al. Insulin-like growth factor 1 promotes proliferation and invasion of papillary thyroid cancer through the STAT3 pathway. *J Clin Lab Anal.* 2020;34(12):e23531.
- Zhang P, Zhang H, Dong W, et al. IL-34 is a potential biomarker for the treatment of papillary thyroid cancer. *J Clin Lab Anal.* 2020;34(8):e23335.
- Feng K, Ma R, Li H, et al. Upregulated SLC27A2/FATP2 in differentiated thyroid carcinoma promotes tumor proliferation and migration. *J Clin Lab Anal.* 2021:e24148.
- Shan S, Wang Y, Zhu C. A comprehensive expression profile of tRNA-derived fragments in papillary thyroid cancer. *J Clin Lab Anal.* 2021;35(3):e23664.
- Toraih EA, Elshazli RM, Trinh LN, et al. Diagnostic and prognostic performance of liquid biopsy-derived exosomal microRNAs in thyroid cancer patients: a systematic review and meta-analysis. *Cancers.* 2021;13(17):4295.
- Qiao DH, He XM, Deng X, et al. Aberrant expression of five miRNAs in papillary thyroid carcinomas. *J Clin Lab Anal.* 2021;35(9):e23907.
- Toraih EA, Fawzy MS, Hussein MH, et al. MicroRNA-based risk score for predicting tumor progression following radioactive iodine ablation in well-differentiated thyroid cancer patients: a propensity-score matched analysis. *Cancers (Basel).* 2021;13(18):4649.
- Schmitt AM, Chang HY. Long noncoding RNAs in cancer pathways. *Cancer Cell.* 2016;29(4):452-463.
- Gao N, Li Y, Li J, et al. Long non-coding RNAs: the regulatory mechanisms, research strategies, and future directions in cancers. *Front Oncol.* 2020;10:598817.
- Qian Y, Shi L, Luo Z. Long non-coding RNAs in cancer: implications for diagnosis, prognosis, and therapy. *Front Med (Lausanne).* 2020;7:612393.
- Yang JP, Yang XJ, Xiao L, Wang Y. Long noncoding RNA PVT1 as a novel serum biomarker for detection of cervical cancer. *Eur Rev Med Pharmacol Sci.* 2016;20(19):3980-3986.
- Yu J, Han J, Zhang J, et al. The long noncoding RNAs PVT1 and uc002mbe.2 in sera provide a new supplementary method for hepatocellular carcinoma diagnosis. *Medicine (Baltimore).* 2016;95(31):e4436.
- Xun C, Jiang D, Tian Z, Yunus A, Chen J. Long noncoding RNA plasmacytoma variant translocation gene 1 promotes epithelial-mesenchymal transition in osteosarcoma. *J Clin Lab Anal.* 2021;35(1):e23587.
- Zeng C, Yu X, Lai J, Yang L, Chen S, Li Y. Overexpression of the long non-coding RNA PVT1 is correlated with leukemic cell proliferation in acute promyelocytic leukemia. *J Hematol Oncol.* 2015;8:126.
- Takahashi Y, Sawada G, Kurashige J, et al. Amplification of PVT-1 is involved in poor prognosis via apoptosis inhibition in colorectal cancers. *Br J Cancer.* 2014;110(1):164-171.
- Huang C, Yu W, Wang Q, et al. Increased expression of the lncRNA PVT1 is associated with poor prognosis in pancreatic cancer patients. *Minerva Med.* 2015;106(3):143-149.
- Posa I, Carvalho S, Tavares J, Grosso AR. A pan-cancer analysis of MYC-PVT1 reveals CNV-unmediated deregulation and poor prognosis in renal carcinoma. *Oncotarget.* 2016;7(30):47033-47041.
- Liu E, Liu Z, Zhou Y. Carboplatin-docetaxel-induced activity against ovarian cancer is dependent on up-regulated lncRNA PVT1. *Int J Clin Exp Pathol.* 2015;8(4):3803-3810.
- Riquelme E, Suraokar MB, Rodriguez J, et al. Frequent coamplification and cooperation between C-MYC and PVT1 oncogenes promote malignant pleural mesothelioma. *J Thorac Oncol.* 2014;9(7):998-1007.
- Zhuang C, Li J, Liu Y, et al. Tetracycline-inducible shRNA targeting long non-coding RNA PVT1 inhibits cell growth and induces apoptosis in bladder cancer cells. *Oncotarget.* 2015;6(38):41194-41203.
- Huang XM, Shi SS, Jian TM, Tang DR, Wu T, Sun FY. lncRNA PVT1 knockdown affects proliferation and apoptosis of uveal melanoma cells by inhibiting EZH2. *Eur Rev Med Pharmacol Sci.* 2019;23(7):2880-2887.
- Wei Y, Zhang X. Transcriptome analysis of distinct long non-coding RNA transcriptional fingerprints in lung adenocarcinoma and squamous cell carcinoma. *Tumour Biol.* 2016;37(12):16275-16285.
- Lin T, Hou PF, Meng S, et al. Emerging roles of p53 related lncRNAs in cancer progression: a systematic review. *Int J Biol Sci.* 2019;15(6):1287-1298.
- Olivero CE, Martínez-Terroba E, Zimmer J, et al. p53 Activates the long noncoding RNA Pvt1b to inhibit myc and suppress tumorigenesis. *Mol Cell.* 2020;77(4):761-74.
- Du P, Hu C, Qin Y, et al. lncRNA PVT1 mediates antiapoptosis and 5-fluorouracil resistance via increasing Bcl2 expression in gastric cancer. *J Oncol.* 2019;2019:9325407.
- Jiang X, Wang J, Deng X, et al. Role of the tumor microenvironment in PD-L1/PD-1-mediated tumor immune escape. *Mol Cancer.* 2019;18(1):10.
- Tuttle RM, Haugen B, Perrier ND. Updated American joint committee on cancer/tumor-node-metastasis staging system for differentiated and anaplastic thyroid cancer (Eighth Edition): what changed and why? *Thyroid.* 2017;27(6):751-756.
- Abushouk AI, Kattan SW, Ahmed HT, et al. Expression of oncolong noncoding RNA taurine-upregulated gene-1 in colon cancer: A clinical study supported by in silico analysis. *J Can Res Ther.* 2021. Online ahead of print. <https://www.cancerjournal.net/preprintarticle.asp?id=324167>
- Kattan SW, Hobani YH, Shaheen S, et al. Association of cyclin-dependent kinase inhibitor 2B antisense RNA 1 gene expression and rs2383207 variant with breast cancer risk and survival. *Cell Mol Biol Lett.* 2021;26(1):14.
- Bustin SA, Benes V, Garson JA, et al. The MIQE guidelines: minimum information for publication of quantitative real-time PCR experiments. *Clin Chem.* 2009;55(4):611-622.

32. Livak KJ, Schmittgen TD. Analysis of relative gene expression data using real-time quantitative PCR and the 2- $\Delta\Delta$ CT method. *Methods (San Diego, Calif)*. 2001;25(4):402-408.
33. Rashid FA, Tabassum S, Khan MS, et al. VE1 immunohistochemistry is an adjunct tool for detection of BRAF. *J Clin Lab Anal*. 2021;35(2):e23628.
34. Schraders M, de Jong D, Kluin P, Groenen P, van Krieken H. Lack of Bcl-2 expression in follicular lymphoma may be caused by mutations in the BCL2 gene or by absence of the t(14;18) translocation. *J Pathol*. 2005;205(3):329-335.
35. Berntsson J, Eberhard J, Nodin B, Leandersson K, Larsson AH, Jirstrom K. Expression of programmed cell death protein 1 (PD-1) and its ligand PD-L1 in colorectal cancer: relationship with sidedness and prognosis. *Oncoimmunology*. 2018;7(8):e1465165.
36. Shan T, Chen S, Wu T, Yang Y, Li S, Chen X. PD-L1 expression in colon cancer and its relationship with clinical prognosis. *Int J Clin Exp Pathol*. 2019;12(5):1764-1769.
37. Peng X, Zhang K, Ma L, Xu J, Chang W. The role of long non-coding RNAs in thyroid cancer. *Front Oncol*. 2020;10:941.
38. Zhou Q, Chen J, Feng J, Wang J. Long noncoding RNA PVT1 modulates thyroid cancer cell proliferation by recruiting EZH2 and regulating thyroid-stimulating hormone receptor (TSHR). *Tumour Biol*. 2016;37(3):3105-3113.
39. Colombo T, Farina L, Macino G, Paci P. PVT1: a rising star among oncogenic long noncoding RNAs. *Biomed Res Int*. 2015;2015:304208.
40. Wang D, Hu Y. Long non-coding RNA PVT1 competitively binds MicroRNA-424-5p to regulate CARM1 in radiosensitivity of non-small-cell lung cancer. *Mol Ther Nucleic Acids*. 2019;16:130-140.
41. Chen J, Yu Y, Li H, et al. Long non-coding RNA PVT1 promotes tumor progression by regulating the miR-143/HK2 axis in gallbladder cancer. *Mol Cancer*. 2019;18(1):33.
42. Zhang R, Li J, Yan X, et al. Long noncoding RNA plasmacytoma variant translocation 1 (PVT1) promotes colon cancer progression via endogenous sponging miR-26b. *Med Sci Monit*. 2018;24:8685-8692.
43. Yu X, Zhao J, He Y. Long non-coding RNA PVT1 functions as an oncogene in human colon cancer through miR-30d-5p/RUNX2 axis. *J BUON*. 2018;23(1):48-54.
44. Guo J, Hao C, Wang C, Li L. Long noncoding RNA PVT1 modulates hepatocellular carcinoma cell proliferation and apoptosis by recruiting EZH2. *Cancer Cell Int*. 2018;18:98.
45. Xu Y, Luo X, He W, et al. Long non-coding RNA PVT1/miR-150/HIG2 axis regulates the proliferation, invasion and the balance of iron metabolism of hepatocellular carcinoma. *Cell Physiol Biochem*. 2018;49(4):1403-1419.
46. Guan Y, Kuo WL, Stilwell JL, et al. Amplification of PVT1 contributes to the pathophysiology of ovarian and breast cancer. *Clin Cancer Res*. 2007;13(19):5745-5755.
47. Yang Q, Yu Y, Sun Z, Pan Y. Long non-coding RNA PVT1 promotes cell proliferation and invasion through regulating miR-133a in ovarian cancer. *Biomed Pharmacother*. 2018;106:61-67.
48. Wang W, Zhou R, Wu Y, et al. PVT1 promotes cancer progression via MicroRNAs. *Front Oncol*. 2019;9:609.
49. Onagoruwa OT, Pal G, Ochu C, Ogunwobi OO. Oncogenic role of PVT1 and therapeutic implications. *Front Oncol*. 2020;10:17.
50. Wu Q, Yang F, Yang Z, et al. Long noncoding RNA PVT1 inhibits renal cancer cell apoptosis by up-regulating Mcl-1. *Oncotarget*. 2017;8(60):101865-101875.
51. Tang J, Li Y, Sang Y, et al. LncRNA PVT1 regulates triple-negative breast cancer through KLF5/beta-catenin signaling. *Oncogene*. 2018;37(34):4723-4734.
52. Feng K, Liu Y, Xu LJ, Zhao LF, Jia CW, Xu MY. Long noncoding RNA PVT1 enhances the viability and invasion of papillary thyroid carcinoma cells by functioning as ceRNA of microRNA-30a through mediating expression of insulin like growth factor 1 receptor. *Biomed Pharmacother*. 2018;104:686-698.
53. Enumah S, Fingeret A, Parangi S, Dias-Santagata D, Sadow PM, Lubitz CC. BRAF. *World J Surg*. 2020;44(8):2685-2691.
54. Yoon H, He H, Nagy R, et al. Identification of a novel noncoding RNA gene, NAMA, that is downregulated in papillary thyroid carcinoma with BRAF mutation and associated with growth arrest. *Int J Cancer*. 2007;121(4):767-775.
55. Wang Q, Yang H, Wu L, et al. Identification of specific long non-coding RNA expression: profile and analysis of association with clinicopathologic characteristics and BRAF mutation in papillary thyroid cancer. *Thyroid*. 2016;26(12):1719-1732.
56. Song B, Li R, Zuo Z, et al. LncRNA ENST00000539653 acts as an oncogenic factor via MAPK signalling in papillary thyroid cancer. *BMC Cancer*. 2019;19(1):297.
57. Esposito R, Esposito D, Pallante P, Fusco A, Ciccodicola A, Costa V. Oncogenic properties of the antisense lncRNA. *Cancer Res*. 2019;79(9):2124-2135.
58. Rusinek D, Swierniak M, Chmielik E, et al. BRAFV600E-associated gene expression profile: early changes in the transcriptome, based on a transgenic mouse model of papillary thyroid carcinoma. *PLoS One*. 2015;10(12):e0143688.
59. Vousden KH, Prives C. Blinded by the light: the growing complexity of p53. *Cell*. 2009;137(3):413-431.
60. Jin K, Wang S, Zhang Y, et al. Long non-coding RNA PVT1 interacts with MYC and its downstream molecules to synergistically promote tumorigenesis. *Cell Mol Life Sci*. 2019;76(21):4275-4289.
61. Manzella L, Stella S, Pennisi MS, et al. New insights in thyroid cancer and p53 family proteins. *Int J Mol Sci*. 2017;18(6):1325.
62. Chiappetta G, Valentino T, Vitiello M, et al. PATZ1 acts as a tumor suppressor in thyroid cancer via targeting p53-dependent genes involved in EMT and cell migration. *Oncotarget*. 2015;6(7):5310-5323.
63. Zhang J, Cao M, Dong J, et al. ABRO1 suppresses tumourigenesis and regulates the DNA damage response by stabilizing p53. *Nat Commun*. 2014;5:5059.
64. Read ML, Seed RI, Fong JC, et al. The PTTG1-binding factor (PBF/PTTG1IP) regulates p53 activity in thyroid cells. *Endocrinology*. 2014;155(4):1222-1234.
65. Prodosmo A, Giglio S, Moretti S, et al. Analysis of human MDM4 variants in papillary thyroid carcinomas reveals new potential markers of cancer properties. *J Mol Med (Berl)*. 2008;86(5):585-596.
66. Gupta A, Jain S, Khurana N, Kakar AK. Expression of p63 and Bcl-2 in malignant thyroid tumors and their correlation with other diagnostic immunocytochemical markers. *J Clin Diagn Res*. 2016;10(7):EC04-EC08.
67. Pilotti S, Collini P, Rilke F, Cattoretti G, Del Bo R, Pierotti MA. Bcl-2 protein expression in carcinomas originating from the follicular epithelium of the thyroid gland. *J Pathol*. 1994;172(4):337-342.
68. Visco C, Wang J, Tisi MC, et al. Hepatitis C virus positive diffuse large B-cell lymphomas have distinct molecular features and lack BCL2 translocations. *Br J Cancer*. 2017;117(11):1685-1688.
69. Chung YL, Sheu ML, Yen SH. Hepatitis C virus NS5A as a potential viral Bcl-2 homologue interacts with Bax and inhibits apoptosis in hepatocellular carcinoma. *Int J Cancer*. 2003;107(1):65-73.
70. D'Andr ea G, Lassalle S, Guevara N, Mograbi B, Hofman P. From biomarkers to therapeutic targets: the promise of PD-L1 in thyroid autoimmunity and cancer. *Theranostics*. 2021;11(3):1310-1325.
71. Chowdhury S, Veyhl J, Jessa F, et al. Programmed death-ligand 1 overexpression is a prognostic marker for aggressive papillary thyroid cancer and its variants. *Oncotarget*. 2016;7(22):32318-32328.
72. Fu G, Polyakova O, MacMillan C, Ralhan R, Walfish PG. Programmed death - ligand 1 expression distinguishes invasive encapsulated follicular variant of papillary thyroid carcinoma from noninvasive follicular thyroid neoplasm with papillary-like nuclear features. *EBioMedicine*. 2017;18:50-55.
73. Shi RL, Qu N, Luo TX, et al. Programmed death-ligand 1 expression in papillary thyroid cancer and its correlation with clinicopathologic factors and recurrence. *Thyroid*. 2017;27(4):537-545.

74. Ahn S, Kim TH, Kim SW, et al. Comprehensive screening for PD-L1 expression in thyroid cancer. *Endocr Relat Cancer*. 2017;24(2):97-106.
75. Chintakuntlawar AV, Rumilla KM, Smith CY, et al. Expression of PD-1 and PD-L1 in anaplastic thyroid cancer patients treated with multimodal therapy: results from a retrospective study. *J Clin Endocrinol Metab*. 2017;102(6):1943-1950.
76. Lubin D, Baraban E, Lisby A, Jalali-Farahani S, Zhang P, Livolsi V. Papillary thyroid carcinoma emerging from hashimoto thyroiditis demonstrates increased PD-L1 expression, which persists with metastasis. *Endocr Pathol*. 2018;29(4):317-323.
77. Gillanders SL, O'Neill JP. Prognostic markers in well differentiated papillary and follicular thyroid cancer (WDTC). *Eur J Surg Oncol*. 2018;44(3):286-296.
78. Aghajani MJ, Yang T, McCafferty CE, Graham S, Wu X, Niles N. Predictive relevance of programmed cell death protein 1 and tumor-infiltrating lymphocyte expression in papillary thyroid cancer. *Surgery*. 2018;163(1):130-136.
79. An HJ, Ko GH, Lee JH, et al. Programmed death-ligand 1 expression and its correlation with lymph node metastasis in papillary thyroid carcinoma. *J Pathol Transl Med*. 2018;52(1):9-13.
80. Shi X, Yu PC, Lei BW, et al. Association between programmed death-ligand 1 expression and clinicopathological characteristics, structural recurrence, and biochemical recurrence/persistent disease in medullary thyroid carcinoma. *Thyroid*. 2019;29(9):1269-1278.
81. Ulisse S, Tuccilli C, Sorrenti S, et al. PD-1 ligand expression in epithelial thyroid cancers: potential clinical implications. *Int J Mol Sci*. 2019;20(6):1405.
82. Zhou L, Cha G, Chen L, Yang C, Xu D, Ge M. HIF1 α /PD-L1 axis mediates hypoxia-induced cell apoptosis and tumor progression in follicular thyroid carcinoma. *Oncotargets Ther*. 2019;12:6461-6470.
83. Dong P, Xiong Y, Yue J, Hanley SJB, Watari H. Tumor-intrinsic PD-L1 signaling in cancer initiation, development and treatment: beyond immune evasion. *Front Oncol*. 2018;8:386.

SUPPORTING INFORMATION

Additional supporting information may be found in the online version of the article at the publisher's website.

How to cite this article: Ibrahiem AT, Makhdoom AK, Alanazi KS, et al. Analysis of anti-apoptotic PVT1 oncogene and apoptosis-related proteins (p53, Bcl2, PD-1, and PD-L1) expression in thyroid carcinoma. *J Clin Lab Anal*. 2022;36:e24390. doi:[10.1002/jcla.24390](https://doi.org/10.1002/jcla.24390)